

# Onset of superconductor-insulator transition in an ultrathin NbN film under in-plane magnetic field studied by terahertz spectroscopy

M. Šindler<sup>1,\*</sup>, F. Kadlec<sup>1</sup>, and C. Kadlec<sup>1</sup>  
<sup>1</sup>*Institute of Physics, Czech Academy of Sciences,  
 Na Slovance 2, 182 21 Prague 8, Czech Republic*  
 (Dated: 1st Sept, 2021)

Optical conductivity of a moderately disordered superconducting NbN film was investigated by terahertz time-domain spectroscopy in external magnetic field applied along the film plane. The film thickness of about 5 nm was comparable with the coherence length, so vortices should not form. This was confirmed by the fact that no marked difference between the spectra with terahertz electric field set perpendicular and parallel to the external magnetic field was observed. Simultaneous use of Maxwell-Garnett effective medium theory and the model of optical conductivity by Herman and Hlubina proved to correctly reproduce the terahertz spectra obtained experimentally in a magnetic field of up to 7 T. This let us conclude that the magnetic field tends to suppress the superconductivity, resulting in an inhomogeneous state where superconducting domains are enclosed within a normal-state matrix. The scattering rate due to pair-breaking effects was found to linearly increase with magnetic field.

PACS numbers: 74.25.Gz, 74.25.N-, 74.78.Db

## I. INTRODUCTION

In superconducting materials, the interactions between external static magnetic field and charge carriers are of fundamental importance. Magnetic field induces screening currents (orbital effect), and it interacts with the electron spin (Zeeman effect). Screening currents usually suppress the magnetic field in the bulk, so the Zeeman effect is weakened. However, in-plane magnetic field will fully penetrate films whose thickness is much lower than the penetration depth  $\lambda$ ; therefore, the Zeeman effect can be dominant. In case of low spin-orbit scattering, magnetic field shifts the density of states (DOS) of electrons with spins up and down by  $\pm\mu_B\mu_0H$ , where  $H$  is the magnetic field intensity,  $\mu_0$  is the permeability of free space and  $\mu_B = 9.274 \times 10^{-24} \text{ J} \cdot \text{T}^{-1}$  denotes the Bohr magneton. The spin-orbit scattering leads to spin flipping, and the spectroscopic gap  $\Omega_G$  is reduced by  $2\mu_B\mu_0H$ . As the spin-orbit scattering rate increases, peaks in the DOS due to up and down spins are smeared and, eventually, only one broad peak in the DOS remains. The spin-orbit scattering rate is proportional to the fourth power of atomic number. Therefore, low spin-orbit scattering is typical of atoms with a low atomic number, which was confirmed by observations in Al films [1]. The field also breaks the time-reversal symmetry, causing an overall weakening of the superconducting state. Abrikosov and Gorkov derived a theory describing superconductivity in the presence of magnetic impurities involving a pair-breaking parameter  $\alpha$  [2]. Later, Maki [3] and de Gennes [4] proved that all ergodic pair-breaking perturbations contribute to the pair-breaking parameter  $\alpha$ . This applies also to ultrathin superconducting films—those having a thickness

comparable with or smaller than the coherence length—in the dirty limit, exposed to either in-plane or out-of-plane magnetic fields. These become effectively two-dimensional, and an in-plane magnetic field can induce a superconductor-insulator transition (SIT) [5, 6]. The SIT introduces a nanoscale inhomogeneity, causing either an enhancement of Coulombic interactions and a gradual decrease in the superconducting gap energy (fermionic scenario [7]), or a gradual loss of coherence within the condensate (bosonic scenario [8]). Such inhomogeneities were reported for various cases of the SIT [5, 9, 10].

In order to extend the knowledge of the behavior of ultrathin superconducting films, we studied the effects of in-plane magnetic field on the optical conductivity by means of time-domain terahertz (THz) spectroscopy. We employed a custom-made experimental setup with external magnetic field. Our measurements are able to provide access to the features which characterize the superconductivity, namely density of states, quasiparticle and Cooper-pair concentrations, vortex dynamics [11], and mesoscopic inhomogeneity. In the present work, we focus on the thinnest available NbN film from the series studied in Ref. 12 which shows an onset of the SIT.

## II. EXPERIMENT

The film was deposited on a  $10 \times 10 \times 1 \text{ mm}^3$ -sized (100) MgO substrate by reactive magnetron sputtering of a 99.999%-pure Nb target in a mixed Ar / N<sub>2</sub> atmosphere with partial pressures of  $P_{\text{Ar}} = 1.5 \times 10^{-3} \text{ mbar}$  and  $P_{\text{N}_2} = 3.3 \times 10^{-4} \text{ mbar}$ . The substrate holder was heated to 850 °C, and NbN was deposited at a rate of  $\sim 0.12 \text{ nm/s}$ . More details about the deposition technology can be found in Ref. 13. The thickness of our film was determined from the known deposition rate as  $d = 5.3 \text{ nm}$  which is close to the typical coherence length in NbN

\* sindler@fzu.cz

(4–7 nm [14]) and much less than the penetration depth  $\lambda = 2.3 \times 10^{-7}$  m, as estimated from the imaginary part of complex conductivity at low frequencies. The critical temperature  $T_c = 13.9$  K was obtained in an independent DC-resistivity measurement; this value is slightly lower than in the thicker samples from the same series (15.2 K and 15.5 K for 14.5 nm and 30.1 nm thick samples, respectively) [12]. We note that the critical temperature of NbN can reach up to 17.3 K [15].

THz spectroscopy experiments consisted in measuring the sample transmittance using a custom-made time-domain spectrometer. Broadband THz pulses were generated using a Ti:sapphire femtosecond laser (Vitesse, Coherent) and a large-area interdigitated semiconductor emitter (TeraSED, GigaOptics). The sample was placed in an Oxford Instruments Spectromag He-bath cryostat with mylar windows and a superconducting coil, allowing for cooling the sample down to  $T = 2$  K. The Voigt geometry—i.e., external static magnetic field directed along the sample plane—was used, and the magnetic field was varied up to the maximum value of  $\mu_0 H = 7$  T. The electric vector of the linearly polarized THz pulses was set either parallel or perpendicular to  $\mathbf{H}$ . The transmitted time profiles of electric field intensity  $E(t)$  were detected by phase-sensitive electro-optic sampling [16] in a 1 mm thick  $\langle 110 \rangle$  ZnTe crystal. The frequency ( $\nu$ ) dependence of complex transmittance  $\tilde{t}(\nu)$  was evaluated as the ratio between Fourier transforms  $E_s(\nu)$  and  $E_r(\nu)$  of the time profiles transmitted through the sample and a bare MgO reference substrate, respectively; this approach is known to effectively eliminate all instrumental functions. Prior to the numerical computations of the complex conductivity of the film  $\tilde{\sigma}(\nu)$ , interference effects in the MgO substrates were avoided by truncating the measured time profiles  $E(t)$  before the echoes arising from internal reflections, whereas interferences in the thin film were accounted for [17]:

$$\tilde{t}(\nu) = \frac{E_s(\nu)}{E_r(\nu)} = \frac{[1 + \tilde{n}_{\text{sub}}(\nu)] e^{i\psi(\nu)}}{1 + \tilde{n}_{\text{sub}}(\nu) + Z_0 \tilde{\sigma}(\nu) d}, \quad (1)$$

where  $Z_0$  denotes the vacuum impedance,  $\tilde{n}_{\text{sub}}(\nu)$  the complex refractive index of the substrate, and  $\psi(\nu)$  is the phase delay due to different optical thicknesses of the sample and reference. Since, in both these cases, the same substrate material (MgO) was used, we can write

$$\psi(\nu) = \frac{2\pi\nu}{c} [(\tilde{n}(\nu) - 1)d + \tilde{n}_{\text{sub}}(\nu)(d_{\text{sub}} - d_{\text{sub}}^r)], \quad (2)$$

where  $c$  is the light velocity,  $\tilde{n}$  is the complex refractive index of the film,  $d_{\text{sub}}$  and  $d_{\text{sub}}^r$  are the thicknesses of the sample-supporting and reference substrates, respectively. The first term in the square brackets stems from the propagation in the film, and the second one reflects the different thicknesses of the sample and reference substrates.

Alternatively, the complex conductivity of the film in the superconducting state  $\tilde{\sigma}^{\text{sc}}(\nu)$  can be obtained by assuming a precise knowledge of the film conductivity  $\tilde{\sigma}^{\text{n}}(\nu)$

in the normal state just above  $T_c$ . In fact, as one evaluates the ratio of transmittances in the superconducting and normal states using Eq. (1), the numerators cancel out, yielding:

$$\frac{\tilde{t}_{\text{sc}}(\nu)}{\tilde{t}_{\text{n}}(\nu)} = \frac{1 + \tilde{n}_{\text{sub}}(\nu) + Z_0 \tilde{\sigma}^{\text{n}}(\nu) d}{1 + \tilde{n}_{\text{sub}}(\nu) + Z_0 \tilde{\sigma}^{\text{sc}}(\nu) d} \quad (3)$$

from which  $\tilde{\sigma}^{\text{sc}}(\nu)$  can be evaluated. This simplification is possible because the optical properties of the MgO substrate change very weakly within such a narrow temperature interval. As an advantage, this approach is not affected by any inaccuracy in the values of  $d_{\text{sub}}$ ,  $d_{\text{sub}}^r$ . The normal-state conductivity  $\tilde{\sigma}^{\text{n}}(\nu)$  was carefully determined previously [12].

### III. RESULTS AND DISCUSSION

In the present work, the sample was probed by linearly polarized THz pulses in two distinct geometries, with electric field vector  $\mathbf{E}$  parallel and perpendicular to the direction of in-plane magnetic field, which we mark in the following by symbols  $E^{\parallel}$  and  $E^{\perp}$ , respectively. The complex conductivity of the film  $\tilde{\sigma}(\nu)$  was evaluated by the two above-described methods based on Eqs. (1) and (3).

#### A. Zero magnetic field

We start with the analysis of normal-state properties of our ultrathin NbN film. They were found to be accurately described by the Drude model, yielding a DC conductivity of  $\sigma_0 = (1.53 \pm 0.02) \mu\Omega^{-1}\text{m}^{-1}$  and a scattering time  $\tau_{\text{n}} = (15 \pm 8)$  fs [12]. The latter value indicates a moderate disorder, and, in principle, quantum corrections to the Drude model might be applicable [18, 19]. However, Cheng *et al.* [20] systematically studied NbN films with an increasing level of disorder, and quantum corrections appeared to play no significant role in their best-quality samples, exhibiting the highest values of  $T_c$ . Since the value of  $T_c$  in our film even slightly exceeds those reported in Ref. 20, we conclude that quantum corrections need not be taken into account.

In general, it is quite difficult to determine precisely the THz properties of superconducting films. This is especially true of the transmittance phase, because one has to distinguish between the contributions of the thin film and that of the substrate which is much thicker, in our case by more than five orders of magnitude thicker. We optimized the substrate thickness within the experimental accuracy so that THz spectra for  $H = 0$  show no dissipation [ $\sigma_1(\nu) \approx 0$ ] below the optical gap  $2\Delta$  in the zero-temperature limit. This corresponds to the expected behavior. By numerical calculations using Eq. (1), the precise mean value of the substrate thickness was found

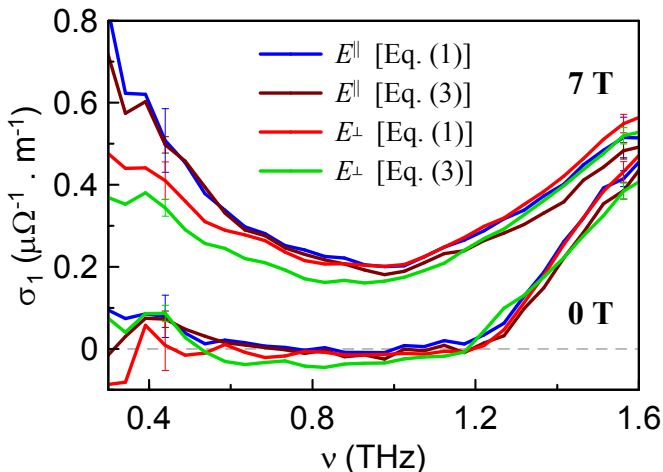


FIG. 1. Real part spectra of NbN conductivity  $\sigma_1(\nu)$  obtained by the two described methods from experiments using both linear polarizations at  $T = 3$  K and a magnetic field of 0 and 7 T. Note that the evaluation of the imaginary part  $\sigma_2(\nu)$  provides spectra with a much lower uncertainty.

as  $d_{\text{sub}} = (990.0 \pm 0.5) \mu\text{m}$ . The alternative method using Eq. (3) lead to the same results, see Fig. 1 ( $\sigma_2(\nu)$  is shown in the Supplemental Material [21]).

At zero magnetic field, the sample conductivity shows features typical of a classical BCS superconductor—below the optical gap  $2\Delta(0)$ , there is no dissipation in the real part, i.e.,  $\sigma_1 \approx 0$ , and a  $1/\nu$  dependence in the imaginary part  $\sigma_2(\nu)$  is observed (see black lines in Fig. 2). At low frequencies,  $\sigma_1 \ll \sigma_2$ ; thus  $\sigma_1$  is determined less reliably than  $\sigma_2$ .

The zero-field conductivity can be best described by the Herman-Hlubina (HH) model for Dynes superconductors [22], see the red lines in Fig. 3. Within this model, the scattering rate in the normal state  $\Gamma_n$  can be written as a sum of two terms related to the superconducting state:  $\Gamma_n = \Gamma_s + \Gamma$  where  $\Gamma_s$  and  $\Gamma$  are the scattering rates relative to the pair-conserving and pair-breaking processes, respectively. The parameter  $\Gamma$  also appears in the well-known Dynes formula [23] where it accounts for the broadening of the DOS which diverges at  $\pm\Delta$  for  $\Gamma = 0$ . The normal-state scattering rate is linked to the scattering time  $\tau_n$  by the relation  $\Gamma_n = (h/2\pi)(2\tau_n)^{-1}$ , where  $h$  is the Planck constant. In the limit  $\Gamma = 0$ , i.e., without pair-breaking processes, the HH model reproduces the Zimmermann model [24] which was successfully applied in the previous report on the ultrathin NbN sample [12]. In the present work, by fitting our zero-field spectra of the complex conductivity  $\tilde{\sigma}(\nu)$  using the HH model, we found  $\Gamma_s/h = (5.6 \pm 0.4)$  THz [25],  $\Gamma/h \leq 10^{-3}$  THz and  $2\Delta(0)/h = 1.2$  THz. Due to the small value of  $\Gamma$ , the Zimmermann model is fully appropriate for the magnetic-field-free case. Indeed, from the values of scattering rates found in the superconducting state, we obtained  $\tau_n = (14 \pm 1)$  fs which is in excellent agreement with the Drude fit of the normal-state spectra reported in Ref. 12. However, unlike the HH model,

the Zimmermann model is not able to account for modifications of the superconducting state due to magnetic field.

## B. Magnetic field dependence

Upon applying the in-plane magnetic field, the complex conductivity is modified, see Fig. 2. Whereas the imaginary-part spectra  $\sigma_2(\nu)$  vary only slightly even for the highest attainable field, the real-part spectra  $\sigma_1(\nu)$  show more significant changes. The dissipation increases with magnetic field; this occurs especially at low frequencies where an upward tail in  $\sigma_1(\nu)$  gradually develops. We did not observe any significant differences between the spectra corresponding to the THz pulses with linear polarizations parallel and perpendicular to the external magnetic field. By contrast, similar experiments with a thicker NbN sample revealed a strongly polarization-dependent transmittance [26]. In the present case, the fact that the spectra for the two THz polarization directions are similar lets us conclude that the NbN sample contains no vortices oriented along the direction of the magnetic field, in contrast to predictions for thicker samples under in-plane applied magnetic field [27]. This is in agreement with our estimate that the coherence length is comparable with the film thickness, thus the vortex cores do not fit in.

Our experimental observations are different from those of Xi *et al.* [14, 28] who reported a prominent decrease in the gap energy upon increasing magnetic field, whereas there was no dissipation below the gap. They employed successfully the model of complex conductivity developed by Skalski *et al.* [29]. Thus, we conclude that this model is not applicable in our case. The NbN sample studied by Xi *et al.* was 70 nm thick, it had a critical temperature of  $T_c = 12.8$  K, and a scattering time of  $\tau_n = 0.07$  fs, two orders of magnitude lower than in the present case. We suppose that the major difference in the spectral responses is linked to the sample thicknesses; whereas the sample in Ref. [28] was much thicker than the typical coherence length, the thickness of our sample was comparable with the coherence length. Consequently, only our sample can be considered as a two-dimensional system.

We assume that upon applying in-plane magnetic field, the superconducting properties are weakened by pair-breaking processes and, additionally, the system becomes inhomogeneous. In such a case, within the film, isolated superconducting islands are formed, surrounded by a matrix in which the superconducting properties are heavily suppressed; this part can be approximated by the normal state. The spectral response of superconducting islands is described by the HH model [22] where  $\Gamma$  plays a role analogous to the pair-breaking parameter  $\alpha$ . We have reproduced the experimental data by the Maxwell-Garnett model [30] in which the superconducting islands were treated as particles and the normal state as a ma-

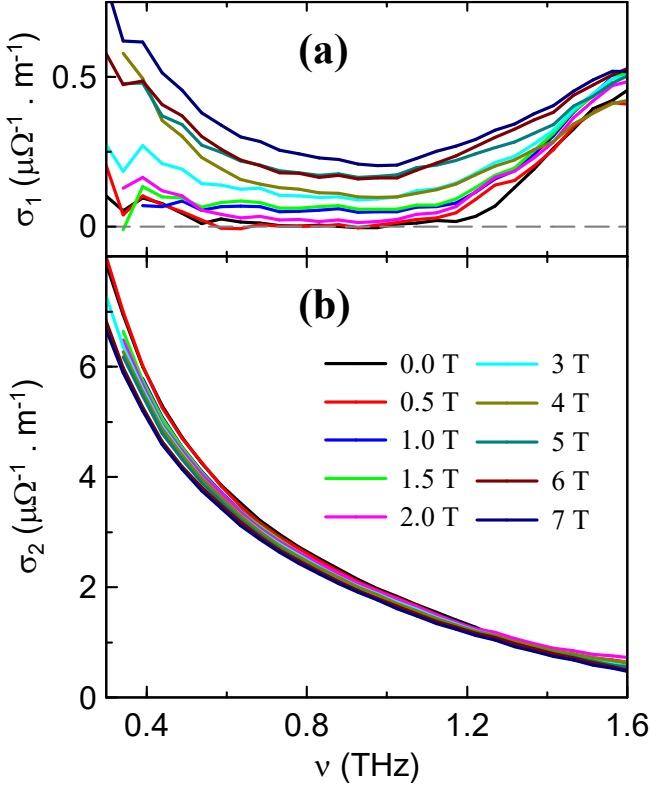


FIG. 2. Real (a) and imaginary (b) part of the conductivity of the NbN film under varying in-plane magnetic field at  $T = 3 \text{ K}$  for  $E^{\parallel}$  evaluated using Eq. (1).

trix [12]:

$$\frac{\tilde{\sigma}_{\text{MG}}(\nu) - \tilde{\sigma}_{\text{n}}(\nu)}{L\tilde{\sigma}_{\text{MG}}(\nu) + (1-L)\tilde{\sigma}_{\text{n}}(\nu)} = f_s \frac{\tilde{\sigma}_{\text{s}}(\nu) - \tilde{\sigma}_{\text{n}}(\nu)}{L\tilde{\sigma}_{\text{s}}(\nu) + (1-L)\tilde{\sigma}_{\text{n}}(\nu)}, \quad (4)$$

where  $f_s$  and  $L$  are the volume fraction and the depolarization factor of the superconducting inclusions, respectively. Although the actual topology of the superconducting film can be non-trivial, we assume the depolarization factor to amount to  $L = 1/3$ . This value is usually employed for calculating the response of flat disks embedded in a matrix, but it may equally describe other geometries.

The use of the Maxwell-Garnett formula for high concentrations of inclusions might be questioned. However, Rychetský *et al.* [31] argued that the Maxwell-Garnett formula holds even for high concentrations of inclusions as long as the matrix is percolated. In our fits, we used two fitting parameters—the volume fraction of superconducting islands  $f_s$ , and the pair-breaking rate  $\Gamma$  which determines the shape of the  $\sigma_s(\nu)$  spectra. In fact, varying  $\Gamma_s$  and  $\Delta$  did not improve our fits, so we conclude that their values are independent of the magnetic field.

Our model describes correctly all observed spectral features, see Fig. 3. THz conductivity spectra for both linear polarizations *evaluated by both methods* were fitted

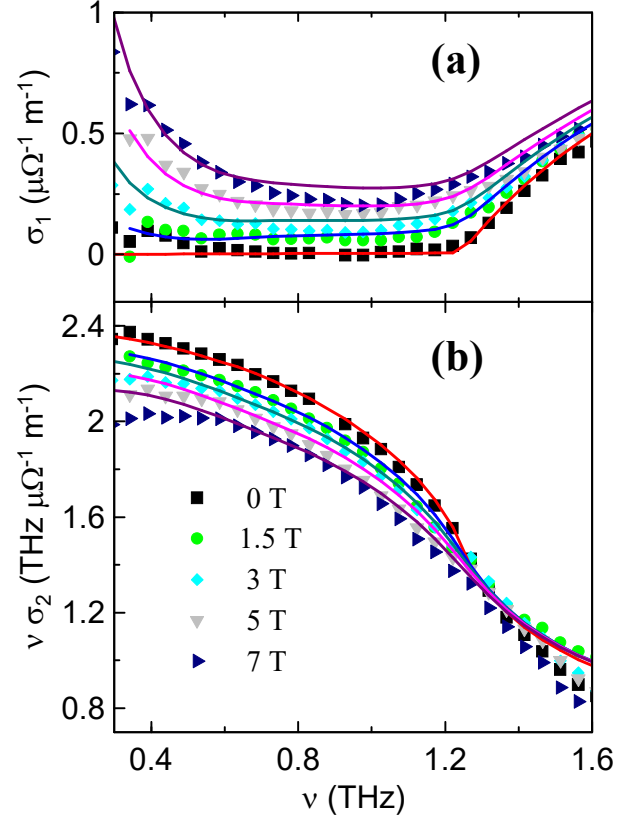


FIG. 3. Symbols: real (a) and imaginary (b) part of the conductivity of NbN at  $T = 3 \text{ K}$  for  $E^{\parallel}$  evaluated using Eq. (1). Lines are fits by the Maxwell-Garnett formula [Eq. (4)] using the Drude model for the normal-state  $\tilde{\sigma}_{\text{n}}(\nu)$  and the HH model for the superconducting-state  $\tilde{\sigma}_{\text{s}}(\nu)$  components, respectively. The imaginary part is plotted as  $\nu\sigma_2(\nu)$  for improved clarity.

using only two free parameters:  $\Gamma$  and  $f_s$ , see Fig. 4. Although there is some scatter in the parameters, their field dependences exhibit clear trends. Whereas the volume fraction of superconducting inclusions  $f_s$  linearly decreases with  $H$  from 1 to 0.94, the pair-breaking scattering rate  $\Gamma$  linearly rises with the magnetic field as  $\Gamma/h = 0.0072 \text{ THz} \cdot \text{T}^{-1} \mu_0 H$ , which corresponds to  $0.5 \mu_B \mu_0 H/h$ . The field-dependences of  $f_s$  and  $\Gamma$  would be qualitatively the same if we assumed different values of  $L$ ; however, the experiment provides no means to obtain its most appropriate value.

The field-dependences  $\Gamma(H)$  of the pair-breaking scattering rate upon a strong spin-orbit interaction were predicted to be quadratic for an in-plane magnetic field and linear for an out-of-plane field [32, 33]. Xi *et al.* [34] performed far-infrared measurements under an in-plane magnetic field, and they evaluated the pair-breaking parameter using the Skalski model [29]. They obtained, in agreement with the theory, a quadratic dependence for a NbTiN thin film, but they also observed a linear behavior for their NbN film with  $\Gamma/h = 0.014 \text{ THz} \cdot \text{T}^{-1} \mu_0/h = \mu_B \mu_0 H/h$ . In contrast with our results, they observed no

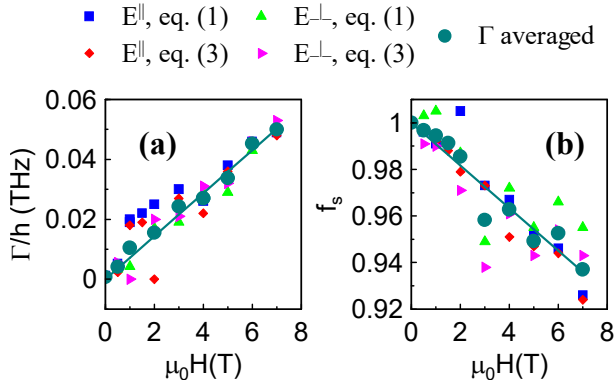


FIG. 4. Symbols: (a) Cooper-pair-breaking scattering rate  $\Gamma$  and (b) volume fraction of superconducting inclusions  $f_s$  obtained from fits of  $\tilde{\sigma}(\nu)$  spectra at  $T = 3$  K, as a function of applied in-plane magnetic field.  $\Gamma$  and  $f_s$  are the only two free parameters of the used Maxwell-Garnett model in combination with the HH and Drude models. Lines: fits demonstrating that both these parameters depend linearly on the magnetic field.

absorption below the optical gap, and they found a linear decrease in the spectroscopic gap  $\Omega_G$  with quite a steep slope of  $-0.12 \text{ THz} \cdot \text{T}^{-1}$  ( $\sim 8.6 \mu_B/h$ ). This is different from the trend observed in our data which revealed only a small decrease in the optical gap even at the magnetic field of 7 T.

We believe that the observed linear dependence  $\Gamma(H)$  is due to a combination of Zeeman splitting of the DOS and the spin-orbit interaction. The peaks in the DOS become doublets due to the Zeeman effect, and they merge into a broad peak with a shape which can be well described by a formula pertinent for a Dynes superconductor.

### C. Temperature dependence under magnetic field

In order to further test the validity of our model, we performed an additional set of measurements. It consisted in setting the magnetic field to the highest attainable value of  $\mu_0 H = 7$  T and measuring the temperature dependence of the conductivity of the NbN film. The experimental results (shown by symbols in Fig. 5) were evaluated from the transmission ratio  $\tilde{t}_{sc}/\tilde{t}_n$  (see Eq. 3) where the normal-state transmittance was measured at  $T = 14.4$  K. In the fitting procedure, in order to account for the effect of heating, we assumed the temperature dependence of the gap in the form [35]

$$\Delta(T) = \Delta(0) \sqrt{\cos \frac{\pi}{2} \left( \frac{T}{T_c} \right)^2}. \quad (5)$$

The scattering rate  $\Gamma$  was assumed to be temperature independent in agreement with previous measurements of different NbN sample [36]. In a MoC film, which is a sim-

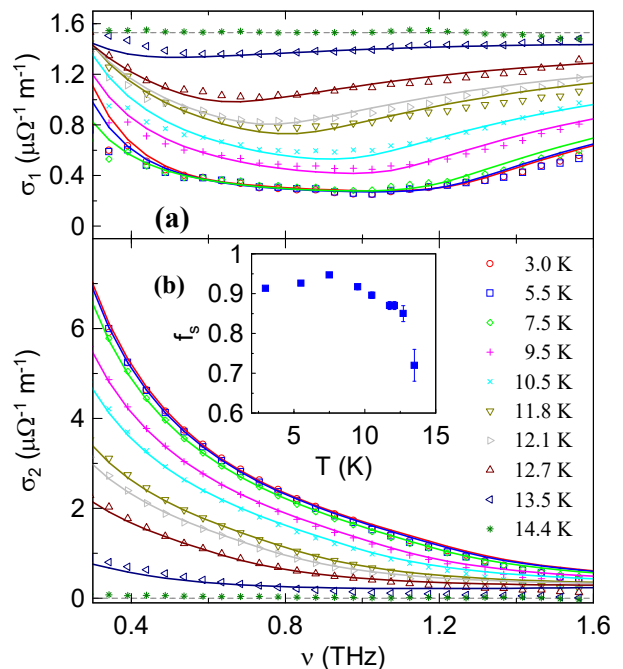


FIG. 5. Symbols: real (a) and imaginary (b) conductivity of NbN at  $\mu_0 H = 7$  T for linear polarization parallel with the external magnetic field evaluated from the transmission ratio  $t_{sc}/t_n$ . Lines: fits using the Maxwell-Garnett [Eq. (4)], HH (Ref. 22), and Drude models. In the fitting, we used a temperature-dependent gap energy  $\Delta(T)$  expressed by Eq. (5), a temperature-independent scattering rate  $\Gamma$ , whereas the superconducting fraction  $f_s(T)$  was used as a free fitting parameter at each temperature. Inset: temperature dependence of the superconducting fraction  $f_s$  obtained from the fits.

ilar superconducting compound,  $\Gamma$  was found to be temperature independent up to  $0.5 T_c$  and at higher temperatures, it reached up to four times the low-temperature value [37]. Our model shows an excellent agreement with the experiment, see Fig. 5. This lets us conclude that at fixed magnetic field of  $\mu_0 H = 7$  T, the superconducting fraction  $f_s$  is only weakly temperature dependent up to  $T = 10$  K, and it sharply decreases upon further heating (see inset of Fig. 5).

## IV. SUMMARY AND CONCLUSION

We studied the optical conductivity of a high-quality ultrathin NbN film under in-plane applied external magnetic field of up to 7 T, in the low-temperature limit. We measured its transmission in the THz range (0.4–1.6 THz), utilizing broadband pulses with linear polarization set either parallel or perpendicular to the applied static magnetic field, and we evaluated the complex conductivity spectra  $\tilde{\sigma}(\nu)$  using two different methods, one based on a direct computation [Eq. (1)] and one employing the ratio between the complex transmittances of the

superconducting and normal states  $\tilde{t}_{sc}(\nu)/\tilde{t}_n(\nu)$  [Eq. (3)]. Both these approaches lead essentially to the same results, as shown in Fig. 1. Nevertheless,  $\tilde{\sigma}(\nu)$  can be determined more precisely by the latter method, since the main source of experimental uncertainty originates in the substrate thickness  $d_{\text{sub}}$  which is effectively canceled in the ratio, and the relative errors in determining conductivity values are lower in the normal state than in the superconducting one.

The zero-magnetic field spectrum is well described by the Zimmermann model [24], as discussed in our previous publication [12]. In the present case, however, we used a more general model—that for Dynes superconductors proposed by Herman and Hlubina [22], which is able to take into account the Cooper-pair-breaking processes. We found that the scattering rates in the normal and the superconducting states are in excellent agreement ( $\Gamma_s = \Gamma_n$ ). The value of  $\Gamma$  is negligibly small, suggesting that Cooper-pair-breaking processes are weak, thus confirming the applicability of the Zimmermann model.

In the low-temperature limit, we observed a significant modification of the conductivity under in-plane magnetic field. Its imaginary part is dominated by the London term,  $\sigma_2(\nu) \sim 1/\nu$ , and it only slightly decreases with  $H$ . The real part  $\sigma_1(\nu)$  exhibits an marked absorption even at frequencies below the optical gap; it does not vanish even at the highest attained magnetic field. We did not observe any relevant difference between the spectra obtained in  $E^{\parallel}$  and  $E^{\perp}$  configurations, unlike in our previous experiments with thicker NbN films [26]. This absence of anisotropy rules out the presence of vortex chains predicted earlier by Luzhbin [27].

We found that our experimental results can be explained by assuming a local suppression of superconducting properties, resulting in an inhomogeneous state of superconducting islands in a normal state matrix with a complex topology. The properties of superconducting islands are modified by pair-breaking effects proportional to the strength of the applied magnetic field. We found that in the present case the HH model for Dynes superconductors [22] is more suitable than the Skalski model [29]. An inhomogeneity on the nanoscale arising owing to the SIT was reported earlier in other cases [5, 9, 10]. In order to quantitatively describe our spectra, we developed a model assuming superconducting islands enclosed within a normal-state matrix, based on the Maxwell-Garnett theory [30]. The complex topology was described by assuming a depolarization factor of  $L = \frac{1}{3}$ . Our model yields a linear decrease in the volume fraction of superconducting islands  $f_s$  with magnetic field. At the same time, we observed a gradual decrease in the superconducting properties of our NbN film, which is reflected by the linear rise in the pair-breaking scattering rate  $\Gamma$  with magnetic field. Finally, our approach has proved to remain valid also for higher temperatures.

## V. ACKNOWLEDGMENT

We are grateful to K. Ilin and M. Siegel for preparing and characterizing the NbN sample as well as to F. Herman and R. Hlubina for fruitful discussions. We also acknowledge the financial support by the Czech Science Foundation (Project No. 21-11089S) and by the MŠMT Project No. SOLID21 – CZ.02.1.01/0.0/0.0/16.019/0000760.

- 
- [1] R. Meservey, P. M. Tedrow, and P. Fulde, *Phys. Rev. Lett.* **25**, 1270 (1970).
- [2] A. Abrikosov and L. Gor'kov, *Zh. Eksp. Teor. Fiz.* **39**, 1781 (1960).
- [3] R. Parks, *Superconductivity: Part 2 (In Two Parts)*, Superconductivity (Taylor & Francis, 1969).
- [4] P. G. de Gennes, *Physik der kondensierten Materie* **3**, 79 (1964).
- [5] V. F. Gantmakher, M. V. Golubkov, V. T. Dolgoplov, A. Shashkin, and G. E. Tsydynzhapov, *J. Exp. Theor. Phys. Lett.* **71**, 473 (2000).
- [6] K. A. Parendo, K. H. S. B. Tan, and A. M. Goldman, *Phys. Rev. B* **73**, 174527 (2006).
- [7] A. Finkelstein, *JETP Lett.* **45**, 46 (1987).
- [8] M. P. A. Fisher, P. B. Weichman, G. Grinstein, and D. S. Fisher, *Phys. Rev. B* **40**, 546 (1989).
- [9] B. Sacépé, C. Chapelier, T. I. Baturina, V. M. Vinokur, M. R. Baklanov, and M. Sanquer, *Phys. Rev. Lett.* **101**, 157006 (2008).
- [10] Y. Noat, V. Cherkez, C. Brun, T. Cren, C. Carbillat, F. Debontridder, K. Ilin, M. Siegel, A. Semenov, H.-W. Hübers, and D. Roditchev, *Phys. Rev. B* **88**, 014503 (2013).
- [11] M. Dressel, *Adv. in Condens. Matt. Phys.* **2013**, 104379 (2013).
- [12] M. Šindler, C. Kadlec, P. Kužel, K. Ilin, M. Siegel, and H. Němec, *Phys. Rev. B* **97**, 054507 (2018).
- [13] D. Henrich, S. Dörner, M. Hofherr, K. Il'in, A. Semenov, E. Heintze, M. Scheffler, M. Dressel, and M. Siegel, *J. Appl. Phys.* **112**, 074511 (2012).
- [14] X. Xi, *Conventional and time-resolved spectroscopy of magnetic properties of superconducting thin films*, dissertation thesis, University of Florida (2011).
- [15] C. P. Poole Jr., H. A. Farach, R. J. Creswick, and R. Prozorov, *Superconductivity* (Academic Press, 2007).
- [16] A. Nahata, J. T. Yardley, and T. F. Heinz, *Appl. Phys. Lett.* **75**, 2524 (1999).
- [17] We are using the convention  $E(t) = E_0 \exp(-i\omega t)$  which implies the following forms of the complex quantities: conductivity  $\tilde{\sigma} = \sigma_1 + i\sigma_2$ , permittivity  $\tilde{\epsilon} = \epsilon_1 + i\epsilon_2$ , and refractive index  $\tilde{n} = n + i\kappa$ .
- [18] B. Alsthuler and A. Aronov, "Electron-electron interactions in disordered systems," (North-Holland, Amsterdam, 1987).
- [19] P. Neilinger, J. Greguš, D. Manca, B. Grančič, M. Kopčík, P. Szabó, P. Samuely, R. Hlubina, and M. Grajcar, *Phys. Rev. B* **100**, 241106 (2019).

- [20] B. Cheng, L. Wu, N. J. Laurita, H. Singh, M. Chand, P. Raychaudhuri, and N. P. Armitage, *Phys. Rev. B* **93**, 180511 (2016).
- [21] See Supplemental Material at -URL-.
- [22] F. Herman and R. Hlubina, *Phys. Rev. B* **96**, 014509 (2017).
- [23] R. C. Dynes, V. Narayanamurti, and J. P. Garno, *Phys. Rev. Lett.* **41**, 1509 (1978).
- [24] W. Zimmermann, E. Brandt, M. Bauer, E. Seider, and L. Genzel, *Physica C: Superconductivity* **183**, 99 (1991).
- [25] Throughout the article we express energy in THz units as it allows for a direct comparison with experimental spectra  $\sigma(\nu)$ . The energy can be calculated by multiplying by Planck constant  $h$ . The scattering time  $\tau$  is related to the energy scale  $E$  by  $E = \hbar/\tau$  where  $\hbar$  is the reduced Planck constant.
- [26] M. Šindler, R. Tesař, J. Koláček, and L. Skrbek, *Physica C: Superconductivity its Applications* **533**, 154 (2017), ninth international conference on Vortex Matter in nanostructured Superconductors.
- [27] D. A. Luzhbin, *Phys. Solid State* **43**, 1823 (2001).
- [28] X. Xi, J. Hwang, C. Martin, D. B. Tanner, and G. L. Carr, *Phys. Rev. Lett.* **105**, 257006 (2010).
- [29] S. Skalski, O. Betbeder-Matibet, and P. R. Weiss, *Phys. Rev.* **136**, A1500 (1964).
- [30] J. C. M. Garnett and J. Larmor, *Philos. Trans. Royal Soc. of London. Series A, Containing Papers of a Mathematical or Phys. Character* **203**, 385 (1904).
- [31] I. Rychetský, M. Glogarová, and V. Novotná, *Ferroelectrics* **300**, 135 (2004).
- [32] M. Tinkham, *Introduction to Superconductivity* (McGraw-Hill, New York, 1996).
- [33] P. Fulde, *Modern Phys. Lett. B* **24**, 2601 (2010).
- [34] X. Xi, J.-H. Park, D. Graf, G. L. Carr, and D. B. Tanner, *Phys. Rev. B* **87**, 184503 (2013).
- [35] T. P. Sheahen, *Phys. Rev.* **149**, 368 (1966).
- [36] M. Šindler, R. Tesař, J. Koláček, P. Szabó, P. Samuely, V. Hašková, C. Kadlec, F. Kadlec, and P. Kužel, *Superconductor Sci. Technol.* **27**, 055009 (2014).
- [37] P. Szabó, T. Samuely, V. Hašková, J. Kačmarčík, M. Žemlička, M. Grajcar, J. G. Rodrigo, and P. Samuely, *Phys. Rev. B* **93**, 014505 (2016).

# Supplemental material: Onset of superconductor-insulator transition in a thin NbN film under in-plane magnetic field studied by terahertz spectroscopy

M. Šindler, F. Kadlec, and C. Kadlec

*Institute of Physics, Academy of Sciences, 16253 Prague 6, Czech Republic*

(Dated: September 1, 2021)

In the paper, we presented our experimental data for either  $E^{\parallel}$  or  $E^{\perp}$  linear polarisation which were evaluated either by using equation (1) or by equation (3) from the paper. Here, we show the complete set of graphs which relates to figures 1-3 from the paper. For further details, see the paper text.



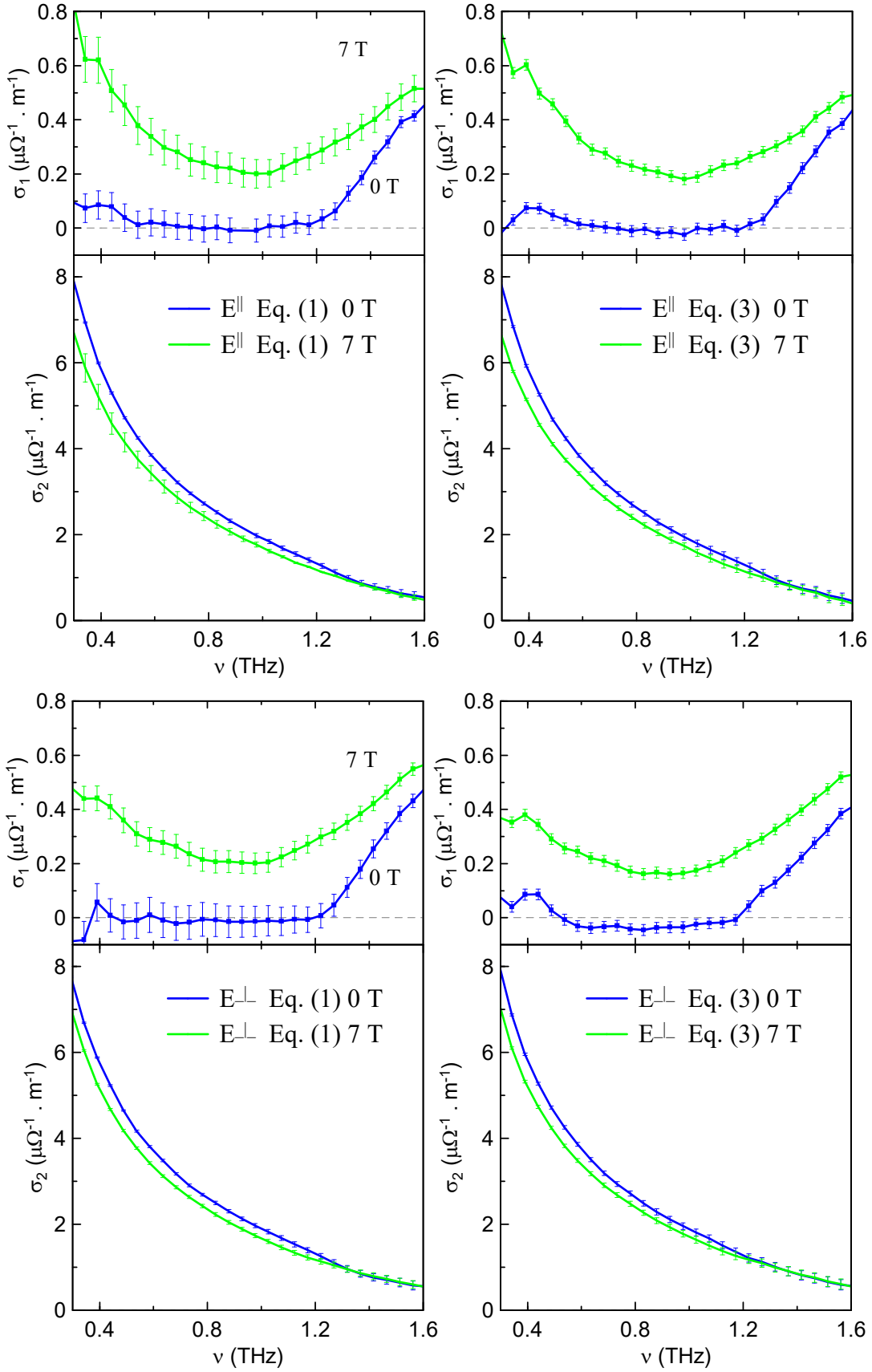


FIG. 1. Real (shown also in the paper) and imaginary part spectra of NbN conductivity  $\sigma_1(\nu)$  together with estimated errorbars for  $E^{\parallel}$  and  $E^{\perp}$  obtained by the two methods described in the paper text at  $T = 3\text{ K}$  and a magnetic field of 0 and 7 T. Note that the evaluation of the imaginary part  $\sigma_2(\nu)$  provides spectra with a much lower uncertainty.

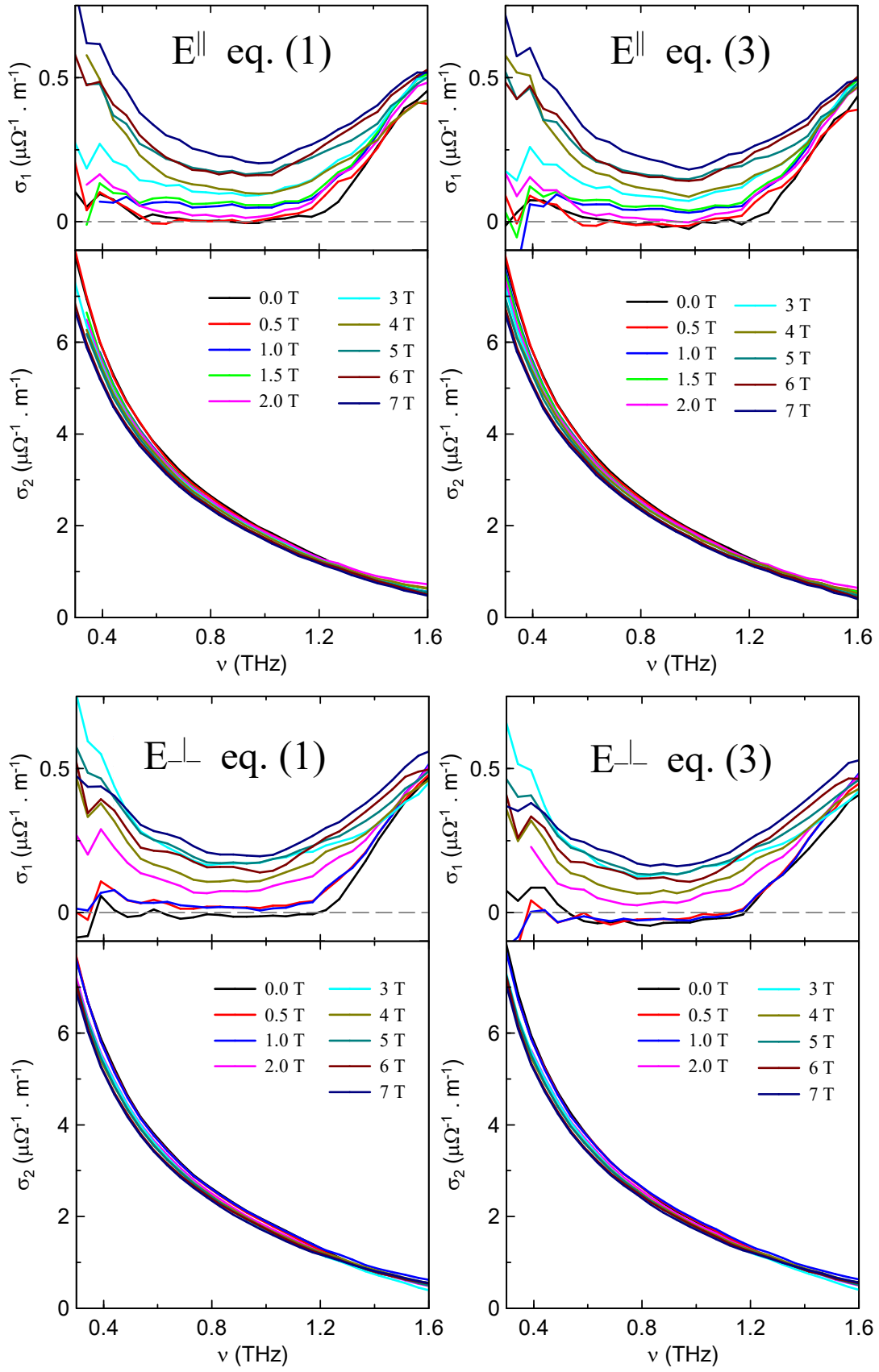


FIG. 2. Real and imaginary part spectra of NbN conductivity  $\sigma(\nu)$  obtained by the two described methods from experiments using both linear polarizations  $E^{\parallel}$  and  $E^{\perp}$  at  $T = 3$  K and a magnetic field from 0 T up to 7 T. Experimental data for  $E^{\parallel}$  and  $E^{\perp}$  are similar, except  $\sigma_1$  for 3 T and  $E^{\perp}$  polarisation which is an outlier deviating from the remaining experiments.

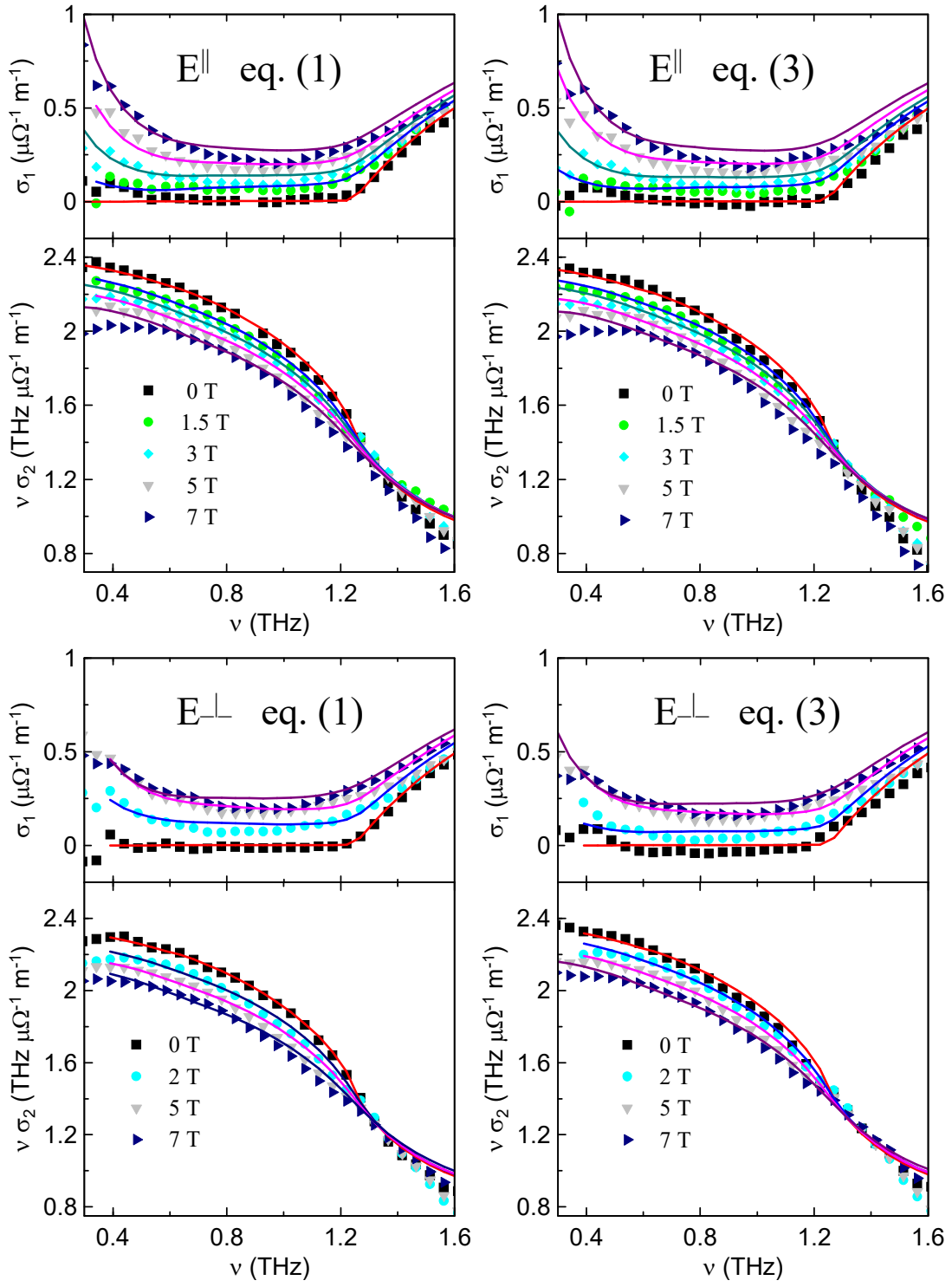


FIG. 3. Symbols: real and imaginary part of the conductivity of NbN at  $T = 3$  K. Lines are fits by the Maxwell-Garnett formula using the Drude model for the normal-state  $\tilde{\sigma}_n(\nu)$  and the HH model for the superconducting-state  $\tilde{\sigma}_s(\nu)$  components, respectively. The imaginary part is plotted as  $\nu\sigma_2(\nu)$  for improved clarity.